

**Dopant enhanced neutralization of low-energy Li<sup>+</sup> scattered from Si(111)**R. D. Gann,<sup>1</sup> Z. Sroubek,<sup>2</sup> and J. A. Yarmoff<sup>1,\*</sup><sup>1</sup>*Department of Physics and Astronomy, University of California, Riverside, California 92521, USA*<sup>2</sup>*Czech Academy of Sciences, Institute of Photonics and Electronics, Chaberska 57, 18251 Prague, Czech Republic*

(Received 10 September 2011; revised manuscript received 19 March 2012; published 12 April 2012)

The neutralization of 3 keV Li<sup>+</sup> ions scattered from Si(111) is measured as a function of doping density, dopant type, and hydrogen coverage. When the surfaces are saturated with hydrogen to unpin the Fermi level, the neutral fractions decrease for lightly doped samples but become anomalously large for highly doped *n*-type Si. A simple model that includes the many-body band-gap narrowing effect predicts the neutralization to good accuracy using a tunneling mechanism similar to the free-electron gas jellium model normally employed for ion/metal interactions, but excluding levels in the gap.

DOI: [10.1103/PhysRevB.85.165307](https://doi.org/10.1103/PhysRevB.85.165307)

PACS number(s): 73.20.At, 34.50.-s, 34.70.+e, 79.20.Rf

**I. INTRODUCTION**

Charge exchange at surfaces is fundamentally important in many physical and chemical processes. Charge exchange influences, among other things, adsorption, etching, oxidation, surface reactions, and vapor deposition. In the dry processing of silicon for microelectronic fabrication, for example, a dependence on doping of oxidation,<sup>1</sup> etching rates,<sup>2</sup> and silicide formation<sup>3</sup> has been observed. To determine how doping-induced electronic structure changes influence these processes requires a basic understanding of how charge exchange at semiconductor surfaces is influenced by doping. For one, the doping concentration changes the density of states at the surface by adding excess majority carriers, which could have a large effect on electron-tunneling rates between reactants and the surface. In addition to populating the bands, the band gap of Si narrows with increasing dopant density,<sup>4</sup> which may also influence charge exchange. Until now, however, no study has been done to clarify if the bulk band gap, rather than the defects and dipole moment induced by the impurities themselves, affects the charge transfer and hence the reaction rates. This aspect of the process is of fundamental scientific and technological importance.

An example of a large effect that doping has in surface reactions is the spontaneous etching of Si by XeF<sub>2</sub> in which the degree and type of dopant affects the reaction rate and the thickness and composition of the resulting surface fluorosilyl layer.<sup>5-8</sup> The reason for the etching rate dependence on doping has been the subject of debate. Excess carriers due to doping may provide nucleation sites for chemical reactants, for example. Another possibility is that the negative F<sup>-</sup> ions formed via tunneling influence band bending at the surface, which in turn affects the mobility of F<sup>-</sup> through the surface fluorosilyl layers. Because of the importance of charge exchange in physical and chemical processes, such as XeF<sub>2</sub> etching, direct measurements of charge exchange at semiconductor surfaces as a function of doping are crucial.

Low-energy ion scattering from surfaces provides a unique test environment for investigating charge exchange and can provide a direct measure of the influence of doping. This technique has shed considerable light on ion yields in secondary-ion mass spectroscopy,<sup>9</sup> stimulated desorption,<sup>10,11</sup> and surface chemical phenomena such as reactivity, selectivity of reactions,<sup>12</sup> and chemisorption. Despite the importance of

semiconductors in materials science and manufacturing, no previous work has directly investigated the effect of the bulk band gap on charge transfer between atomic particles and solid surfaces. Most theoretical analyses of charge exchange during ion scattering, for example, consider the solid to be a free Fermi gas of electrons with a jellium surface. Some recent theoretical<sup>13</sup> and experimental<sup>14</sup> studies have investigated the effects of an anisotropic projected surface band structure on charge transfer, but, again, only for metals.

Silicon provides a system in which the bulk band gap can be altered while retaining the atomic structure and work function, as the (111) face of differently doped samples can be identically prepared as hydrogen-terminated 7×7 surfaces with the Fermi level unpinned. By scattering low-energy ions from hydrogen-terminated Si surfaces as a function of doping, the effects of band-gap magnitude, rather than merely the location of the highest occupied electronic level, can be probed.

Projectiles with low ionization energies or electron affinities (e.g., alkalis, O, and Cu) are best suited for investigations of charge exchange that probe valence states of solids.<sup>15</sup> Li<sup>+</sup> alkali ions are used in the present work because their low mass allows for easy scattering from the relatively light Si atoms, their ionization potential overlaps the filled states in the solid, and the radial symmetry of the 2s ionization level enables a simple analysis. In the low-energy regime (0.5 to 10 keV), the charge transfer to scattered alkali ions is dominated by resonant charge transfer, an efficient one-electron process in which electrons tunnel between the sample and the ion where the energy is degenerate between the two levels.<sup>16</sup> This process is nonadiabatic and the ion-surface interaction results in a significant broadening of the ionization level into a resonance, thus enabling enhanced tunneling into newly available states.

There are dangling bonds on the clean Si(111)-7×7 surface that pin the Fermi level roughly in the middle of the gap<sup>17</sup> and provide electrons that can participate in neutralization that would otherwise not occur.<sup>18</sup> What is not completely clear, however, is which energy levels actually determine the neutralization: the bulk Fermi energy, the surface levels where the Fermi level is pinned, or a mixture of the two due to a transition region. As the surface dangling bonds are passivated, such as by deposition of atomic hydrogen, the Fermi level becomes unpinned,<sup>19</sup> altering the charge transfer significantly. In the case of lightly doped Si(111) and (100), the charge

transfer to scattered  $\text{Li}^+$  ions is suppressed as hydrogen is deposited.<sup>18</sup>

In addition to the influence of dangling bonds, dopant density may also affect charge transfer. In a metal, the neutralization depends principally on the work function of the sample and the ionization level in the projectile atom.<sup>20</sup> Being that the difference in work function between heavily doped and lightly doped Si is only approximately 0.04 eV,<sup>21</sup> very little difference in neutralization probability would be expected. The band gap in Si is narrowed significantly, however, above  $10^{17}$  impurities per  $\text{cm}^3$ . It could be that the overlap of these bands with the ionization level in resonance with the surface bands would then have a large effect on neutralization.

The present work investigates the effect of dopant density and hydrogen adsorption on the neutralization of  $\text{Li}^+$  ions scattered from the H/Si(111)- $7\times 7$  surface. Neutral fractions (NFs) and work functions are measured as the samples are dosed with atomic hydrogen to passivate the dangling bonds. Measurements show that the *n*-type sample with a high dopant density has a large NF, despite nearly identical work functions between lightly and heavily doped samples. A simple flat-band jellium model, excluding states in the gap, is used to predict the NF of the fully passivated surface, and the agreement with the experiment is good. This clearly shows that the bulk band gap has a large effect on ion-surface charge exchange and that the process can be easily modeled.

## II. EXPERIMENTAL PROCEDURE

All samples were prepared by resistive heating to  $1100^\circ\text{C}$  in an ultra-high vacuum (UHV) chamber (base pressure  $3 \times 10^{-10}$  torr), yielding a clean,  $7\times 7$  surface as verified by x-ray photoelectron spectroscopy and low-energy electron diffraction. The (111) surface termination was chosen because of the ease of keeping it atomically clean in UHV over the course of an experiment and because of the relative flatness maintained under hydrogen exposure.<sup>7</sup> We used lightly doped *n*-type (5.0  $\Omega$  cm), lightly doped *p*-type (1.0  $\Omega$  cm), medium-doped *n*-type (0.01  $\Omega$  cm), and heavily doped *n*-type (0.001  $\Omega$  cm) samples.

Atomic hydrogen is produced by backfilling the chamber with  $\text{H}_2$  gas while the sample is held 1 in. away from and facing a hot tungsten filament that cracks the molecules.<sup>22</sup> Doses are given in Langmuirs (1 L =  $10^{-6}$  torr s) of  $\text{H}_2$ , as the actual production rate of atomic H cannot be directly characterized. As the formation of atomic H in this manner is not particularly efficient, 1 L of  $\text{H}_2$  exposure produces much less than one incident hydrogen atom per surface atom. Saturation of the work function occurs at about 1200 L, although data were collected beyond that. Changes in the surface work function with hydrogen exposure are determined from the low-energy cutoff in secondary-electron spectra collected with an electrostatic analyzer (Comstock) while the sample is bombarded by 200 eV electrons.<sup>23</sup>

Time-of-flight (TOF) ion scattering was carried out with a pulsed alkali ion gun (Kimball Physics), employing a pulse width of about 20 ns. Scattered species were detected by a triple micro-channel-plate array in a backscattering geometry with a fixed scattering angle of  $150^\circ$ . The entrance to the detector is held at ground potential to ensure an equal sensitivity to

ions and neutrals.<sup>24</sup> The times measured between pulses on the detector and beam pulse were histogrammed to produce a TOF spectrum. The sample was positioned so that the ions reaching the detector were emitted along the surface normal. The detector leg is equipped with deflection plates that can deflect all ions, allowing separate collection of the total and neutral yield. The deflection plates were cycled every 60 s during data collection so that any slow drifts in ion current did not affect the measured neutral fractions. To calculate a NF, the area of the single-scattering peak in the neutral yield spectrum is divided by that of the total yield spectrum.<sup>25</sup>

## III. RESULTS AND DISCUSSION

Measurements of the work function and NF collected as the samples are dosed with hydrogen are displayed in Fig. 1. Error bars for the NF are assumed to go as the square root of the peak intensity, i.e., the shot noise standard deviation of the single scattering peak. It should be noted that additional error due to differences in sample preparation are likely present, but upon collection of multiple scans were not evident when compared with the statistical noise. The data show that the NF and work functions collected from the two clean surfaces are nearly identical. As hydrogen passivates the surface, the Fermi level becomes unpinning, and the work function decreases (for

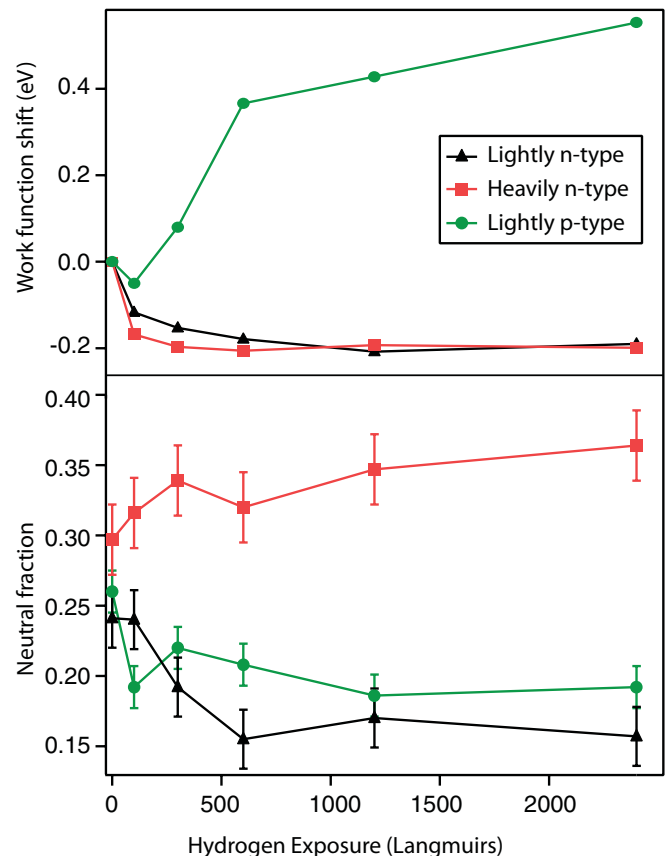


FIG. 1. (Color online) Work-function shifts (top panel) and neutral fractions of scattered 3 keV  $\text{Li}^+$  (bottom panel) for Si(111) surfaces of various doping levels as a function of exposure to atomic H. The data are plotted with respect to the measured dose of  $\text{H}_2$ , which is proportional to the actual atomic H exposure (see text).

$n$  type) or increases (for  $p$  type) to match the bulk value. This is due to the fact that the pinned Fermi level on the clean Si(111)- $7\times 7$  surface is 0.63 eV above the valence-band maximum,<sup>17</sup> nearly in the middle of the gap. This dependence of the work function on doping type indicates that the hydrogen adsorption is indeed unpinning the Fermi level. The values for NF shown in the bottom panel of Fig. 1 do not, however, follow the work-function trends. Instead, lightly doped samples of either dopant type have a similar NF to each other, decreasing from about 25 to 18%, whereas the heavily  $n$ -doped samples were flat or marginally increasing in the range of 30 to 35%, a result which is statistically significant. The fully passivated medium-doping value (not shown) was intermediate to these two values (see Fig. 3). The clean, pinned surface has a neutral fraction that is nearly independent of doping, at a value of about 25 to 27%.

There are several factors that combine in determining the NF for scattered alkalis. When the projectile is far from the surface, the vacant  $s$  level is sharp and located at the ionization energy, but it shifts up when approaching the surface due to the electrostatic image potential. At the same time, the atomic wave function admixes with the wave functions of electrons in the solid, broadening the ionization level. As such, these experiments can determine whether the band gap measurably affects the admixing of atomic and surface electronic states. If the density of states in the gap were truly zero, a dependence of the neutralization probability on doping would be expected, provided that most of the neutralization involves electrons in that energy range.

In order to build a simple model of neutralization of  $\text{Li}^+$  scattered from Si, it is necessary to specify the energy levels of the substrate and of the Li ion, the incoming and outgoing velocity of the Li, and the time-dependent interaction between the Li projectile and the substrate. Our analysis is based on a jellium model of the substrate that has been successfully implemented for a quantitative interpretation of measured NFs<sup>26</sup> in the past. We focus only on the passivated surface without dangling-bond surface states. The interacting atom is described by its ionization level  $\psi_a$ , its ionization energy  $\epsilon_a$ , and the virtual linewidth  $\Delta$ , each as functions of distance from the surface. The energy  $\epsilon_a$  is the sum of the free-atom ionization energy and the image charge shift saturated at the jellium boundary, and the value of  $\Delta$  is determined by the jellium electron density. The substrate energy levels are described by their energy  $\epsilon_k$  and the wave functions  $\psi_k$ . A microscopic model of  $\Delta$  relates the broadening and the electron transfer-matrix element  $V_{ak}$  between  $\psi_k$  and  $\psi_a$  via the approximate independent-particle golden rule formula  $V_{ak}^2 \cong \Delta_a/\pi\rho$ , where  $\rho$  is the density of electronic states of the substrate.  $V_{ak}$  is taken as independent of  $k$  and is, essentially, together with  $\epsilon_a$ , the only parameter in the theoretical description of charge transfer in the low-energy regime. This model agrees very well with experimental data for Li scattered from Cu with  $V_{ak}$  and  $\epsilon_a$  deduced from the jellium model and using  $r_s = 2.8$  au for the electron-gas radius.<sup>27</sup>

For Li scattered from Si, it is possible to approximate  $V_{ak}$  and  $\epsilon_a$  by substituting for the corresponding jellium. Since the electron-gas radius of Si,  $r_s = 2$ , is similar to the  $r_s = 2$  to 2.8 used by Marston *et al.* for Li scattered from Al,<sup>27,28</sup> we use

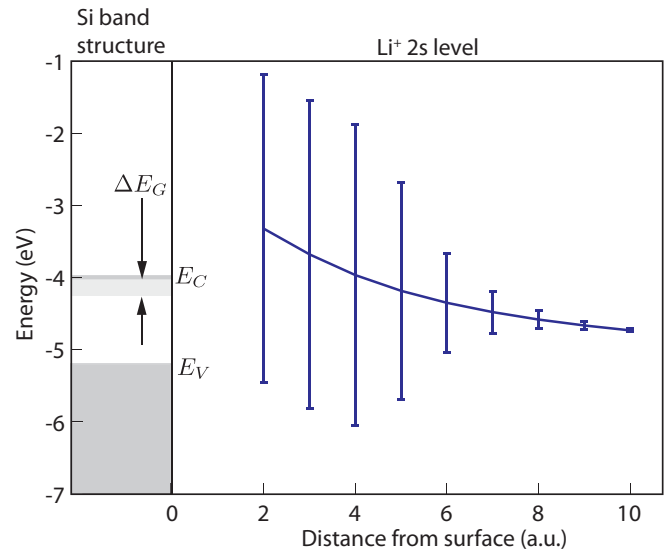


FIG. 2. (Color online) Right: the level position and broadening of the Li  $2s$  as the projectile approaches the surface. Left: a schematic of the band structure of fully passivated Si, illustrating the change in band gap with increased doping.

their values for  $V_{ak}$  and  $\epsilon_a$ . The substrate is specified by the energy distribution of substrate  $k$  levels.

As doping is increased, the band gap between  $E_C$  and  $E_G$  is reduced, as calculated by Lanyon and Tuft,<sup>4</sup> according to

$$\begin{aligned} \Delta E_G &= (3q^2/16\pi\epsilon) \cdot (q^2n/\epsilon kT)^{1/2} \\ &= 22.5(n/10^{18})^{1/2} \text{ meV} \end{aligned} \quad (1)$$

for nondegenerate majority carriers, where  $n$  is the concentration of dopants in cubic centimeters,  $\epsilon$  is the permittivity, and  $q$  is the electron charge. This fits the observed gap width data in the literature and is the same for  $n$ -type or  $p$ -type Si at room temperature. The narrowing is attributed to the interaction of minority carriers with several majority carriers, reducing the barrier to exciton formation. The broadened and shifted level overlaps the surface levels at the point where the effective conduction-band edge moves in response to these carriers. This suggests that there will be an observable change in the neutral fraction due to the band-gap narrowing. For simplicity, we let the band-gap narrowing lower the conduction-band edge in the calculation. The model takes into account the change of NF with surface electronic structure by including more occupied levels in the conduction band as the doping is increased. A precise determination of the energies of these levels is not of particular importance because the energies of these levels are strongly dynamically perturbed.

The level shift and broadening for Li is shown schematically as a function of distance from the surface in Fig. 2 alongside a schematic Si band diagram. This figure shows the Li  $2s$  level position and width as it approaches the surface from the right, as calculated by Marston [Eq. (6) in Ref. 27]. On the left is the approximate band structure of passivated bulk-terminated Si. We take the top of the valence band to be at  $-5.20$  eV, the conduction-band edge to be at  $-4.02$  eV, and an intrinsic band-gap value to be 1.18 eV. Note that the level barely overlaps the valence band at 2 a.u. ( $\approx 1$  Å) from the surface. The lower dark gray area illustrates valence levels

that are populated regardless of doping (though in principle they are slightly depleted in hole doping), and the upper dark gray area illustrates the (very small) populated conduction band at 300 K for the lightly doped samples. The light gray region at the left of Fig. 2 depicts the additional occupied levels that result from band-gap narrowing. Denoted  $\Delta E_G$ , it is drawn for the case of the heavily doped sample, where the effective conduction-band edge is lowered to  $-4.24$  eV. The energy levels illustrated in light gray, which overlap the broadened ionization level, would thus substantially change the neutralization probability by introducing more available tunneling states, particularly given the small amount of overlap with the valence band.

To quantitatively predict the expected NF, we consider a wave function  $|\phi(t)\rangle$  of the Li-Si system composed of the Si wave functions  $|\psi_k\rangle$  in the bands around the gap and the atomic level  $|\psi_a\rangle$ :

$$|\phi(t)\rangle = \sum_k b_k(t) |\psi_k(r)\rangle + b_a(t) |\psi_a(r)\rangle, \quad (2)$$

where  $k$  runs over all levels in the solid under consideration. Referenced to the vacuum, energy levels are counted from the (arbitrary) value of  $-9.13$  eV to the valence-band edge at  $-5.17$  eV and then from the conduction-band minimum, as calculated from Ref. 4, to the vacuum level. For no band narrowing, the conduction-band edge is taken to be at  $-4.01$  eV. Insertion of Eq. (2) into the Schrödinger equation gives a set of differential equations:

$$\begin{cases} i \frac{db_a}{dt} = \sum_k b_k V_{ak} + b_a \epsilon_a, \\ i \frac{db_k}{dt} = b_a V_{ak} + b_k \epsilon_k. \end{cases} \quad (3)$$

To calculate the NF of Li at the end of the scattering process, the independent-particle approximation of the many-body problem is used, based on the solution to the Heisenberg equations of motion, which has been shown to provide NFs that are in good agreement with the experiment for alkalis scattered from metal surfaces.<sup>28,29</sup> The solution of the time-dependent coefficients of the operators is equivalent to the solution of Eq. (3) for  $b(t)$ . For the initial prepared state that has the atomic level vacant and Si levels occupied up to the Fermi energy, the value of the NF is given by  $\text{NF} = \sum |b_k(\infty)|^2$ , where the summation is over all occupied states. The values of  $V_{ak}$  and  $\epsilon_a$  and their time dependence are taken from Ref. 27, with  $V_{ak}$  slightly larger by a factor of 1.4 to fit the asymptotic data for zero doping. Because of the dynamical nature of the scattering, the states in the Si broaden due to the uncertainty principle by  $\alpha v$ , where  $2/\alpha v$  is the time constant of the decay of  $V_{ak}$ . The experimental and theoretical NFs for different dopings are shown in Fig. 3. The model predicts the NF of doped Si to a good degree of accuracy, slightly underestimating for low to intermediate doping and very slightly overestimating for high doping. The resulting theoretical curve, it should be noted, is not the best regression fit to the data but rather one that fits well while still being derived from a physical argument, namely, the jellium model of a substrate interacting with an atomic level. A precise comparison of the shape of the NF dependence with the experiment would not be justified in this case, due to the persistent inhomogeneity in the surface passivation, which

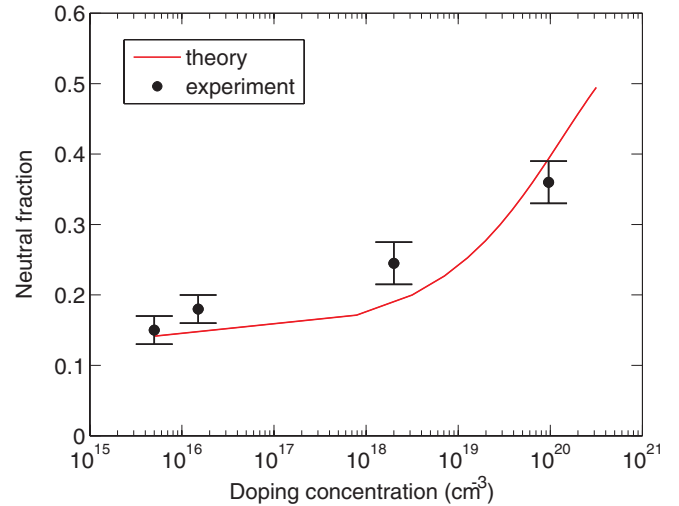


FIG. 3. (Color online) Measured neutral fractions (filled circles) for 3 keV  $\text{Li}^+$  scattered from  $n$ -type Si(111) with a saturation coverage of H, shown along with the neutral fraction predicted by the solution to Eq. (3) (solid line), plotted as a function of dopant concentration.

may contribute to some amount of error in the experimental data.

The simplest explanation for the marginal deviation is inhomogeneity in the hydrogenated surface. The evolution of the  $7 \times 7$  surface as atomic hydrogen is dosed has been studied extensively.<sup>22</sup> Although quoted exposure figures are not directly comparable, the “fully passivated” dosages in this work are well beyond those in the literature at which steady state is reached. For such large exposures, the surface is etched by atomic hydrogen and a steady-state population of monohydrides, dihydrides, and trihydrides is established, along with some newly created dangling bonds.<sup>30</sup> Ideally, a passivated (111) surface would be entirely composed of monohydrides, but this is not attainable on the (111)- $7 \times 7$  surface. The persistent inhomogeneity, and therefore incomplete unpinning of the Fermi surface, will lead to saturation values that are a mixture of the predicted fully passivated values and those associated with a surface pinned by dangling-bond states. Nominally, the pinned surface gives a NF around 27% under these scattering conditions. Thus, if some population of dangling bonds still exists, the predicted value will be too small for the low doping sample, and too large for the high doping samples, as observed.

#### IV. CONCLUSIONS

We have shown how the charge exchange between low-energy alkali ions and silicon surfaces depends on the degree of doping. The neutral fraction for Li scattered from H/Si(111) changes markedly with doping level, due to the band-gap narrowing, while leaving the work function virtually unchanged. This can be understood qualitatively by considering the admixture of the added levels due to band-gap narrowing interacting with the broadened resonance level of the Li  $2s$  state. A simple model captures the important features of the admixing of states quantitatively, implying that this effect is fundamental to charge exchange between atomic

species and semiconductor surfaces. The agreement between the experimental data and the model is quite good, which supports the notion that the bulk band gap in a semiconductor is a large factor in determining the neutralization. In some sense, the semiconductor can be thought of as a free-electron gas confined to a region with a jellium surface, but with electronic levels missing in the gap. This result suggests that electronic

structure, and not just localized impurity states, affects the formation of ions at the surface and therefore reaction rates in silicon.

#### ACKNOWLEDGMENTS

This material is based upon work supported by the National Science Foundation under Grant No. CHE-1012987.

\*yarmoff@ucr.edu

- <sup>1</sup>B. E. Deal and M. Sklar, *J. Electrochem. Soc.* **112**, 430 (1965).
- <sup>2</sup>H. Geng, *Semiconductor Manufacturing Handbook* (McGraw-Hill, Upper Saddle River, 2005).
- <sup>3</sup>R. A. Levy, *Reduced Thermal Processing for ULSI* (Plenum, Murray Hill, 1990).
- <sup>4</sup>H. P. D. Lanyon and R. A. Tuft, *IEEE Trans. Elec. Dev.* **26**, 1014 (1979).
- <sup>5</sup>H. F. Winters and D. Haarer, *Phys. Rev. B* **36**, 6613 (1987).
- <sup>6</sup>F. A. Houle, *J. Appl. Phys.* **60**, 3018 (1986).
- <sup>7</sup>H. F. Winters and J. W. Coburn, *Surf. Sci. Rep.* **14**, 162 (1992).
- <sup>8</sup>J. A. Yarmoff and F. R. McFeely, *Phys. Rev. B* **38**, 2057 (1988).
- <sup>9</sup>H. W. Werner, *Vac.* **24**, 493 (1974).
- <sup>10</sup>M. Szymonski, J. Kolodziej, Z. Postawa, P. Czuba, and P. Piatkowski, *Prog. Surf. Sci.* **48**, 83 (1995).
- <sup>11</sup>J. Lee, Z. Zhang, and J. T. Yates, Jr., *Phys. Rev. B* **79**, 081408 (2009).
- <sup>12</sup>J. C. Tully, *Ann. Rev. Phys. Chem.* **51**, 153 (2000).
- <sup>13</sup>E. A. Carter, K. Niedfeldt, and P. Nordlander, *Surf. Sci.* **600**, L291 (2006).
- <sup>14</sup>A. Schmitz, J. Shaw, H. S. Chakraborty, and U. Thumm, *Phys. Rev. A* **81**, 042901 (2010).
- <sup>15</sup>B. J. Garrison, A. C. Diebold, J. H. Lin, and Z. Sroubek, *Surf. Sci.* **124**, 461 (1983).
- <sup>16</sup>J. J. C. Geerlings, L. F. T. Kwakman, and J. Los, *Surf. Sci.* **184**, 305 (1987).
- <sup>17</sup>F. J. Himpsel, G. Hollinger, and R. A. Pollak, *Phys. Rev. B: Condens. Matter* **28**, 7014 (1983).
- <sup>18</sup>Y. Yang and J. A. Yarmoff, *Phys. Rev. Lett.* **89**, 196102 (2002).
- <sup>19</sup>F. J. Himpsel, *Surf. Sci.* **299**, 525 (1994).
- <sup>20</sup>J. Los and J. J. C. Geerlings, *Phys. Rep. Rev. Sec. Phys. Lett.* **190**, 133 (1990).
- <sup>21</sup>C. J. Karlsson, E. Landemark, L. S. O. Johansson, U. O. Karlsson, and R. I. G. Uhrberg, *Phys. Rev. B* **41**, 1521 (1990).
- <sup>22</sup>J. J. Boland, *Adv. Phys.* **42**, 129 (1993).
- <sup>23</sup>H. E. Bauer and H. Seiler, *Surf. Interface Anal.* **12**, 119 (1988).
- <sup>24</sup>M. Barat, J. C. Brenot, J. A. Fayeton, and Y. J. Picard, *Rev. Sci. Instrum.* **71**, 2050 (2000).
- <sup>25</sup>C. B. Weare and J. A. Yarmoff, *Surf. Sci.* **348**, 359 (1996).
- <sup>26</sup>P. Nordlander and J. C. Tully, *Phys. Rev. B* **42**, 5564 (1990).
- <sup>27</sup>A. V. Onufriev and J. B. Marston, *Phys. Rev. B* **53**, 13340 (1996).
- <sup>28</sup>J. B. Marston, D. R. Andersson, E. R. Behringer, B. H. Cooper, C. A. DiRubio, G. A. Kimmel, and C. Richardson, *Phys. Rev. B* **48**, 7809 (1993).
- <sup>29</sup>R. Brako and D. M. Newns, *Surf. Sci.* **108**, 253 (1981).
- <sup>30</sup>U. Jansson and K. J. Uram, *J. Chem. Phys.* **91**, 7978 (1989).